INL/RPT-25-84086-Revision-0

Dynamics modeling of molten salt reactor with reduced and expanded representations of delayed neutron precursors

August 2025

Piyush Sabharwall

Changing the World's Energy Future

INL is a U.S. Department of Energy National Laboratory operated by Battelle Energy Alliance, LLC

INL/RPT-25-84086-Revision-0

Dynamics modeling of molten salt reactor with reduced and expanded representations of delayed neutron precursors

Piyush Sabharwall

August 2025

Idaho National Laboratory
Idaho Falls, Idaho 83415

http://www.inl.gov

Prepared for the
U.S. Department of Energy
Under DOE Idaho Operations Office
Contract DE-AC07-05ID14517

Dynamics modeling of molten salt reactor with reduced and expanded representations of delayed neutron precursors

Thabit Abuqudaira[a,*], Pavel Tsvetkov[a], Piyush Sabharwall[b]

[a]Department of Nuclear Engineering, Texas A&M University, 423 Spence St, College Station, TX 77843,

[b]Nuclear Science & Technology, Idaho National Laboratory, 1955 N Fremont Ave, Idaho Falls, ID 83415,

Abstract

Molten salt reactors (MSRs) present unique challenges in dynamic behavior due to the mobility of their fuel. In these reactors, delayed neutron precursors (DNPs) drift with the fuel circulation through the primary loop. As a result, a fraction of DNPs decays outside the core, effectively reducing the available delayed neutron population for reactivity control. Consequently, precise modeling of the distribution and behavior of DNPs is critical for accurate reactor dynamics simulations. In this study, the System Dynamics Analysis Tool (SDAT) was used to simulate a thermal-spectrum MSR under steady-state conditions and following transients. The effects of using reduced and expanded representations of DNPs with fewer or more groups than the conventional 6-group model were investigated. Their impact on the simulated distribution of precursors in the primary loop, reactivity loss value, and reactor response to transients was analyzed. Simulation results showed that reduced models lead to the loss of the actual DNPs distribution data, resulting in less accurate estimates of reactivity loss. Reactor power predictions using these reduced models showed significant deviations compared to those using the conventional 6-group model in transient simulations. Expanded models offered a more accurate representation of the distribution of DNPs

and reactivity loss estimates. Reactor power predictions using expanded models showed minimal deviation from the conventional 6-group model during the simulated transients.

1. Introduction

About 271 nuclides produced from fission have been identified as delayed neutron precursors (DNPs) (Brady, 1989). DNPs are fission fragments or daughters of fission fragments whose beta decay yields a daughter nucleus, which subsequently decays via neutron emission (Duderstadt and Hamilton, 1976). These neutrons emitted after a time delay from the fission process are called delayed neutrons. Delayed neutrons, though constituting a small fraction of the total neutrons produced by fission, are essential for maintaining the stability of the reactor. They slow the rate of reactivity changes, providing a time delay that enhances control and prevents rapid, potentially unsafe reactor power fluctuations (Hetrick, 1971). Accurately representing delayed neutron data is essential for reliable reactor simulations and effective prediction and control of reactor operating conditions.

The molten salt reactor (MSR) is an advanced reactor design expected to play a key role in meeting the growing global demand for clean, sustainable, and safe energy solutions (LeBlanc, 2010). It was chosen as one of the six reactors proposed by the GEN IV International Forum for the next generation of nuclear reactors (Serp et al., 2014). In liquid-fueled MSRs, the nuclear fuel is dissolved in molten salt, acting as both the fuel and the coolant (Riley et al., 2019; Wooten and Powers, 2018). These MSRs allow online refueling, enabling extended operation and better fuel utilization while enhancing safety through passive mechanisms such as freeze plugs (Wu et al., 2022). Additionally, they improve waste management by efficiently burning actinides and allowing the continuous removal of fission products, thereby reducing long-lived radioactive waste

(Elsheikh, 2013; McIntyre et al., 2013). Therefore, there has been a growing trend toward MSR development, with several research projects and demonstration efforts initiated worldwide (Abuqudaira et al., 2023).

However, MSRs present unique challenges in reactor dynamics due to the mobility of their fuel (Brown et al., 2020; Huff, 2019). Unlike solid-fueled reactors, where DNPs remain stationary within the fuel matrix, MSRs experience DNPs drift as the fuel circulates through the primary loop (Krepel et al., 2008). This drift leads to the removal of DNPs from the reactor core. Depending on their half-lives, these DNPs may decay while circulating through the loop or survive long enough to reenter the reactor core. Therefore, the removal and addition of DNPs in and out of the core are influenced by the loop configuration and the flow rate in the primary loop. These unique characteristics of liquid-fueled MSRs make accurate DNPs data even more crucial for understanding and predicting reactor behavior during normal and abnormal conditions.

Previous research on the effects of delayed neutron data on reactor dynamics has provided valuable insights into the complex interplay between this data and the simulated reactor response. Jo et al. (2022) examined the impact of delayed neutron data on dynamic reactivity in light water reactors. Simulation results emphasized the importance of accurate delayed neutron group data for reliable reactor safety analysis. Leconte et al. (2024) have identified inconsistencies in delayed neutron data across different nuclear data libraries, which can influence the calculated kinetic parameters and overall reactor dynamics, underscoring the need for precise and consistent delayed neutron data. Furthermore, (Zuo et al. (2022) developed the ThorCORE3D code to model the flow field effects of DNPs in liquid-fueled MSRs, revealing that the external loop recirculation time and fuel salt flow rate significantly impact the delayed neutron fraction and, consequently, the simulated reactor power and temperature. Collectively, these studies highlight the critical role of

delayed neutron data in enhancing the accuracy of reactor dynamics simulations. However, there is a lack of research on the impact of DNPs models on reactor dynamics, particularly regarding their effect on reactivity loss and transient behavior simulations.

This paper explores the impact of DNPs data on the dynamic response of a thermal-spectrum MSR at steady-state and following transient conditions, focusing on two key aspects. First, it examines the effects of using reduced DNPs models, which consist of fewer than six groups. It evaluates the potential loss of accuracy in reactor dynamics simulations due to this simplification. Second, expanded models incorporating more than six groups are introduced and analyzed to assess their ability to provide a more detailed representation of DNPs behavior and reactor response. These analyses emphasize the critical role of accurate DNPs data in enhancing the fidelity of simulations, improving reactivity loss predictions, and ensuring the safe operation of MSRs, particularly during transient scenarios where precise modeling is crucial.

The paper is organized into five sections. Section 2 introduces the reference MSR design used in the study, describes the loss of DNPs due to fuel salt circulation, and provides an overview of the models of DNPs. Section 3 details the dynamics tool used to track the behavior of DNPs in the primary loop, employing a one-dimensional multi-channel model for simulating the flow and decay of DNPs within the loop. Section 4 presents the research findings from reduced and expanded DNPs models, analyzing their impact on reactor dynamics under steady-state and transient conditions. The distribution of DNPs, their removal, the simulated reactivity loss values, and an extrapolation of the required number of groups to match the experimental reactivity loss value are presented under steady-state conditions. For transient simulations, specifically the reactivity insertion test and the primary pump failure test, the deviations of these models from the conventional 6-group model and their influence on reactor behavior were examined. Finally,

Section 5 summarizes the main conclusions, discusses the implications of the findings, and suggests potential directions for future research.

2. DNPs in MSRs

This section provides an overview of the MSR design utilized in this study, discusses the DNPs loss in this reactor, and describes different modeling approaches for representing DNPs behavior in reactor dynamics simulations.

2.1. Thermal-Spectrum MSR

The Molten Salt Reactor Experiment (MSRE) was used as a reference design in this study due to the availability of design information. In addition, the published experimental data provides a benchmark for validating dynamic models. Its simple and representative configuration as a single-fluid MSR makes it particularly suited for exploring fundamental dynamic behaviors and emerging research topics. It was one of two demonstration reactors built at Oak Ridge National Laboratory as part of the Molten Salt Reactor Program (MSRP) (Abram and Ion, 2008). The MSRE operated for 4.5 years in the 1960s. A detailed description of the reactor design is available in previous studies (Robertson, 1965; Zanetti et al., 2014).

An illustration of the fuel transit time in various primary loop components is shown in Figure 1. In the core, the fuel salt, a mixture of LiF, BeF_2, ZrF_4, ThF_4, and UF_4 salts, circulates in graphite moderator channels. The fuel transit time in the core is τ_C. As the fuel salt exits the reactor core, it passes into the hot leg, spending time in it (τ_{HL}). Then, heat is transferred to a secondary coolant salt, a mixture of LiF and BeF_2 salts, in the heat exchanger. The fuel salt transit time in the tube side of the heat exchanger is τ_H. Eventually, the fuel salt circulates in the cold leg back to the

core. The fuel transit time in the cold leg (including the downcomer) is τ_{CL}. Therefore, the fuel salt transit time in the loop outside the core region (τ_L) is then:

$$\tau_L = \tau_{CL} + \tau_H + \tau_{HL} \quad (1)$$

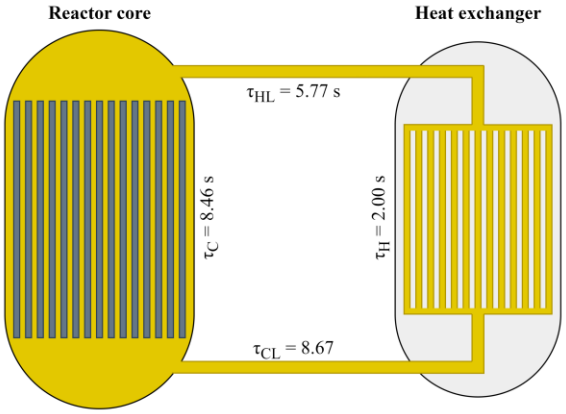

Figure 1. Fuel salt transit times in the primary loop of the MSRE.

2.2. Loss of DNPs

The fuel circulation in MSRs removes a significant fraction of DNPs from the core (Cammi et al., 2012). These removed DNPs may decay, emitting delayed neutrons in the loop outside the reactor core. Thus, there is a reactivity loss due to these lost delayed neutrons (Wooten and Powers, 2018). The degree of reactivity loss strongly depends on the fuel mass flow rate in the primary loop. A higher flow rate increases the fraction of precursors leaving the core before emitting neutrons, thereby decreasing the fraction of delayed neutrons contributing to core reactivity. Conversely, reducing the flow rate allows more precursors to decay within the core, decreasing the reactivity loss.

An early practice in representing DNPs in reactor kinetics calculations is grouping them based on their half-lives into several groups. A six-group representation of DNPs is usually used in reactor kinetics and dynamics studies. The significance of this number of groups is evident from

the insights gained through the kinetic behavior of various chain-reacting systems (Keepin, 1965). The kinetic parameters of the MSRE with ^{233}U as the fissile material are listed in Appendix A, Table A.1. (Steffy R. C. and Wood P. J., 1969). Based on the MSRE design data with six groups of DNPs, the decay probability of precursors of each group is visualized after exiting the core and traveling through the external loop, as shown in Figure 2. It can be observed that the decay probability increases as the fuel salt transit time in the loop increases. In addition, groups with a longer half-life have a lower decay probability, while those with a shorter half-life have a higher decay probability.

In this six-group representation of DNPs, it is apparent that some groups have a significantly shorter half-life than the fuel salt transit time in the loop. Thus, a significant or complete fraction of these DNPs will decay in the loop before the fuel salt reenters the core. However, each group combines several DNPs with an average half-life. Thus, the simulated fraction of DNPs that will decay in the loop outside the core region depends on the number of groups of DNPs and the uncertainty of these data. Therefore, the number of groups utilized in reactor dynamics studies and the uncertainty of these data will play a role in overestimating or underestimating the actual reactor behavior.

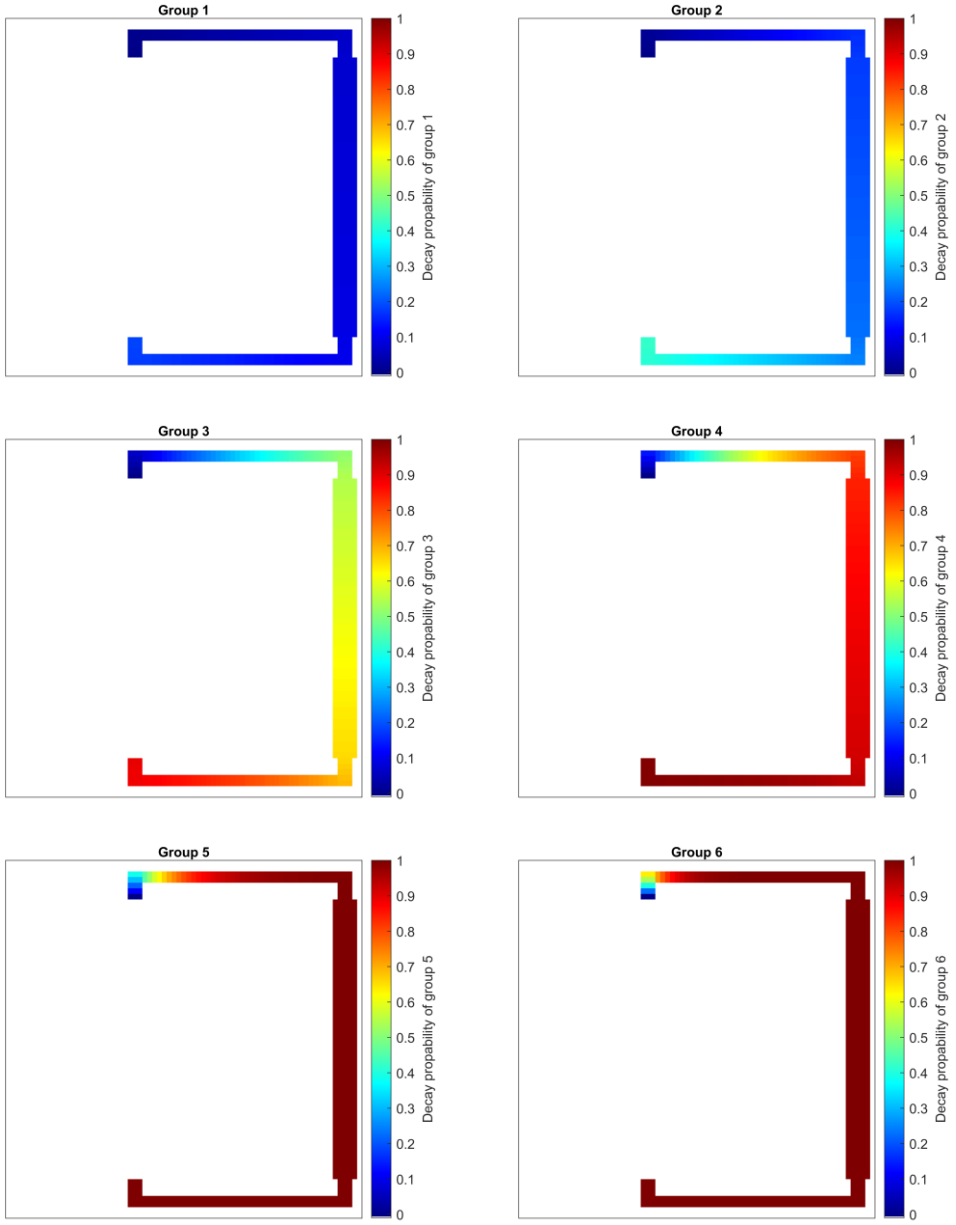

Figure 2. Decay probabilities of DNPs groups in the loop outside the core of the MSRE.

2.3. DNPs Models

Measuring delayed neutron data involves complex and precise techniques, starting with sample irradiation and ending with decay analysis to obtain delayed neutron activity curves (Brady, 1989). Analysis of these curves results in obtaining yields and decay constants, which are fitted into multi-group models, with six groups being the standard choice. Extending the number of

groups requires high-precision data and mathematical techniques to accurately resolve closely spaced decay constants and properly decompose the delayed neutron emission (Tuttle, 1975). Moreover, experimental validation of expanded models becomes increasingly challenging, as distinguishing between groups with similar decay constants introduces additional uncertainties.

This work used the effective delayed neutron data for the MSRE with ^{233}U fissile nuclide to examine the effects of reduced models on the dynamics simulations (Steffy R. C. and Wood P. J., 1969). Reduced models were obtained by group condensation process. The six-group representation provided in Appendix A, Table A.1 was reduced to two-group and single-group models. The condensation process of the six-group model into two-group and single-group models is shown in Figure 3.

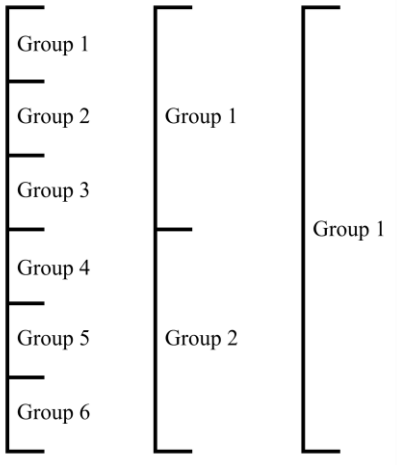

Figure 3. Condensation process of 6-group into 2-group and 1-group DNPs models.

Condensating DNPs groups is a technique that simplifies reactor kinetics calculations by reducing the number of delayed neutron groups. The condensation process ensures that the effective decay constant and effective delayed neutron fraction in the reduced model approximate the original system's behavior. The total effective delayed neutron fraction (β_{eff}) for the reduced model is the sum of the original groups' effective delayed neutron fractions ($\beta_{eff,i}$):

$$\beta_{\text{eff}} = \sum_{i=1}^{G} \beta_{\text{eff},i} \quad (1)$$

The condensation of the decay constant is performed using a weighting function based on either the effective delayed neutron fraction or the concentration of DNPs (C_i). Both approaches result in identical decay constant values:

$$\lambda_{\text{eff}} = \beta_{\text{eff}} \frac{\sum_{i=1}^{G} \lambda_i}{\sum_{i=1}^{G} \beta_{\text{eff},i}} \quad (2)$$

$$\lambda_{\text{eff}} = \frac{\sum_{i=1}^{G} \lambda_i C_i}{\sum_{i=1}^{G} C_i} \quad (3)$$

Detailed 8-group physical data from the thermal neutron fission of ^{233}U, as presented in Appendix A, Table A.2, were used for the dynamic simulation analysis of expanded models (Spriggs et al., 2002). While this data does not contain effective delayed neutron fractions, the physical values of the delayed neutron abundances can be used to find the delayed neutron fractions for each group using the effective delayed neutron fraction for the MSRE design with ^{233}U. The 8-group data was condensed into 7-group and 6-group models to ensure consistency in the comparison. The condensation of groups was performed, ensuring that the resulting groups preserved the total delayed neutron fraction and matched published 7-group and 6-group data in terms of the distribution of groups. The seventh and eighth groups in the 8-group model were condensed into one group in the 7-group model. In addition, the second and third groups in the 7-group model were condensed into one group in the 6-group model. An illustration of the condensation process is shown in Figure 4.

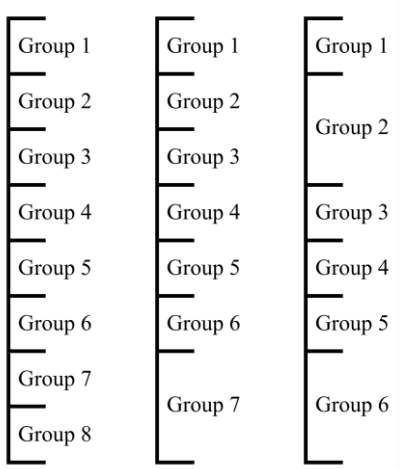

Figure 4. Condensation process of 8-group into 7-group and 6-group DNPs models.

3. System Dynamics Analysis Tool

System Dynamics Analysis Tool (SDAT) was developed for dynamics and stability analysis studies of reactor systems with stationary and flowing fuels. One of its key features is its ability to model the drift of DNPs in MSRs, which is critical for reactor kinetics and stability studies. The tool offers significant advantages in terms of visualization, providing intuitive graphical representations of complex reactor dynamics that enhance user understanding. Its user-friendly interface facilitates seamless interaction with the model, allowing easy input and output data exchange.

SDAT consists of a neutronics model represented by the point reactor kinetics model, a one-dimensional multi-channel thermal-hydraulics model to account for the mass and heat transfer in various reactor components, and a reactivity feedback model. Details on the description of SDAT models and the validation results of reactivity insertion tests conducted at the MSRE are available in previous work (Abuqudaira et al., 2024). In the point reactor kinetics model, a system of equations describes the time-dependent behavior of the neutron density and DNPs densities. The change in neutron density as a function of time can be represented by:

$$\frac{dn(t)}{dt} = \frac{\rho(t)-\beta_{\text{eff}}}{\Lambda} n(t) + \sum_{i=1}^{6} \lambda_i C_i(t) \quad (4)$$

Where $\rho(t)$ is the net reactivity of the core as a function of time, β_{eff} is the effective delayed neutron fraction, Λ is the mean neutron generation time, λ_i is the decay constant for the ith group of DNPs, and $C_i(t)$ is the density of the i^{th} group of DNPs as a function of time. For the system of equations governing the density change of DNPs as a function of time, the conventional set of equations has to be modified to account for the fuel salt circulation and, thus, the loss and addition of DNPs to the core (Macphee, 1958).

In SDAT, the account for the DNPs motion can be modeled through a zero-dimensional or one-dimensional multi-channel model. In the one-dimensional multi-channel model, DNPs are produced from fission in the reactor core, drift through graphite channels, hot leg, tube side of the heat exchanger, and cold leg back to the core channels. The rate of change of group i DNPs density in the r^{th} channel and z^{th} node as a function of time is:

$$\frac{dC_i(t)^{(r,z)}}{dt} = \frac{\beta_{\text{eff},i}}{\Lambda} n(t)^{(r,z)} - \lambda_i C_i(t)^{(r,z)} - \frac{C_i(t)^{(r,z)} - C_i(t)^{(r,z-1)}}{\tau_z} \quad (5)$$

$n(t)^{(r,z)}$ is the one-group neutron density in the r^{th} channel, z^{th} node, and τ_z is the fuel salt transit time in the node. When the fuel salt exits the channels in the reactor core, it will be mixed in the hot leg. Thus, the concentration of the DNPs in the hot leg will be treated as a one-dimensional single-channel model. In addition, one-dimensional single-channel treatment is adapted in the heat exchanger and cold leg. A simplified diagram of the tracking scheme of the DNPs in the primary loop is shown in Figure 5.

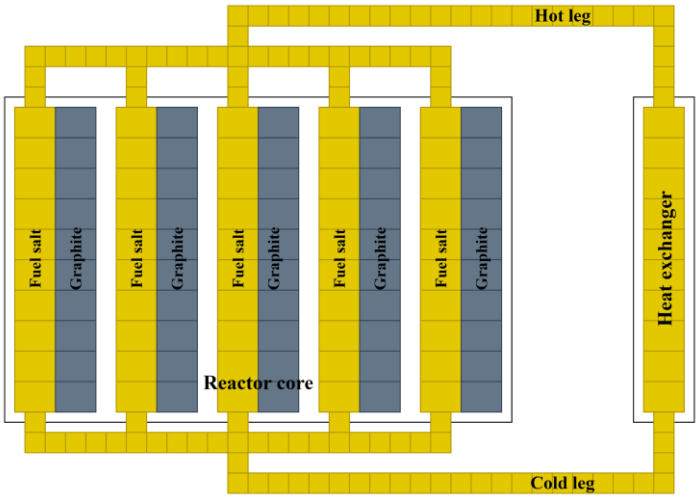

Figure 5. Simplified diagram of the tracking scheme of the DNPs in the primary loop.

4. Results and Discussion

The MSRE operating at a thermal power of 8 MW was simulated in SDAT. In the core, it was reported that 97% of the fission power is deposited in the fuel salt channels, while 3% is in the graphite channels. The spatial power distribution adapted in SDAT was calculated from the reported power distribution for a nine-region MSRE model (Kerlin T. W. et al., 1971). The normalized power distribution in the core channels using SDAT is shown in Figure 6.

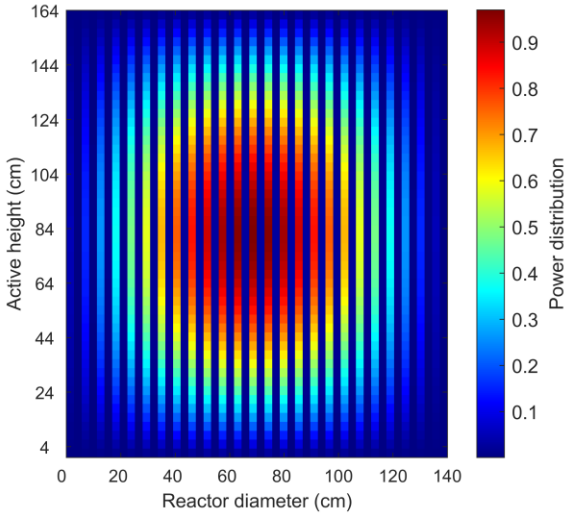

Figure 6. Normalized power distribution in the core channels.

In SDAT, the power distribution in the core channels is used in the thermal-hydraulics model to predict temperature distribution in various reactor components. This model uses reactor thermal power as input from the neutronics model. Thus, the same temperature distribution was obtained at steady-state in all simulations regardless of the implemented model of DNPs. The steady-state temperature distribution in various reactor loops is shown in Figure 7, Figure 8, and Figure 9. The fuel salt temperature increased as it flowed upward through the channels. The central channels exhibited the highest temperatures in the primary loop, attributed to the higher power density at the core center, resulting in more significant heat generation than the outer channels. The fuel salt temperature decreased in the heat exchanger as heat was transferred to the coolant salt in the secondary loop. Subsequently, the coolant salt transferred heat to the air in the tertiary loop, where it was ultimately rejected to the environment.

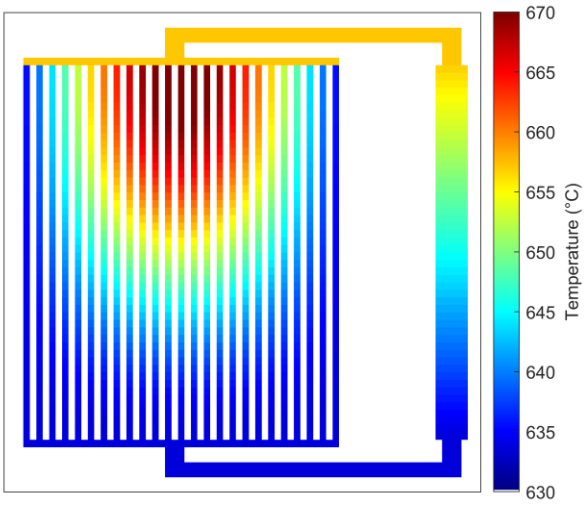

Figure 7. Steady-state temperature distribution in the primary loop (Fuel salt).

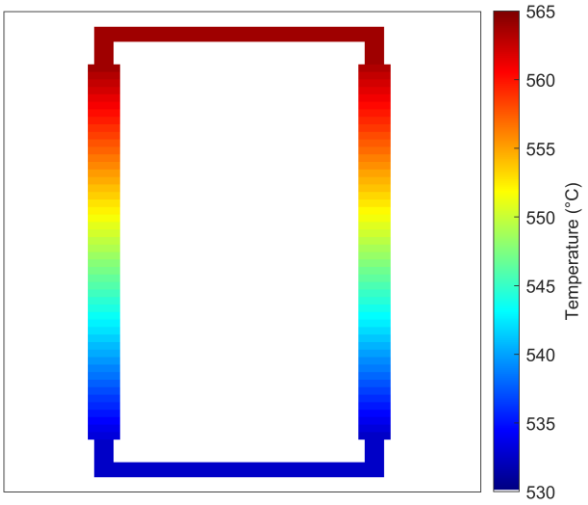

Figure 8. Steady-state temperature distribution in the secondary loop (coolant salt).

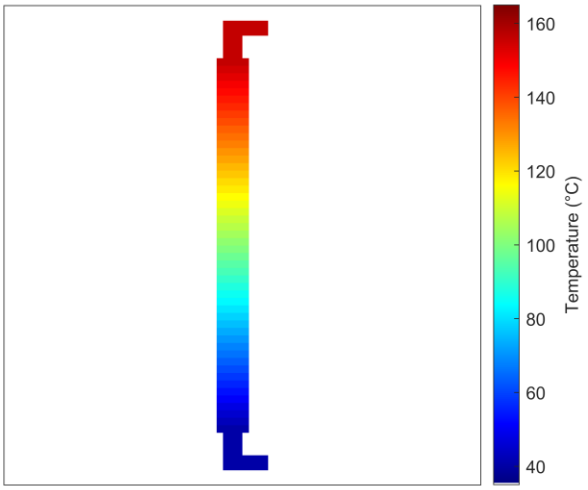

Figure 9. Steady-state temperature distribution in the tertiary loop (air).

Following the steady-state temperature distribution simulation, the influence of using reduced and extended models of DNPs on MSR dynamics simulations was thoroughly examined. The examination included evaluating the estimated distribution of DNPs, reactivity loss due to fuel salt circulation, and the reactor dynamic response to initiated transients.

4.1. Reduced DNPs Models

The impact of implementing two reduced DNPs models was analyzed under both steady-state and transient conditions. These reduced models were created by condensing the standard 6-group representation of DNPs into simplified 2-group and 1-group models within the simulation tool. The analysis focused on assessing the accuracy of the reduced models in predicting the estimated DNPs distribution, reactivity loss value, and overall reactor dynamic behavior in response to transient conditions.

4.1.1. Steady-State

The steady-state normalized concentration of DNPs in the primary loop was simulated for different models, as illustrated in Figure 10, Figure 11, and Figure 12. Normalization was performed by dividing the local concentration at each location by the maximum concentration value. Two main observations were noted using the conventional 6-group representation of DNPs. First, the distribution of groups with the longest half-lives was shifted to the upper part of the core. This tilt is a result of the fuel salt flow in the core. By comparison, the groups with the shortest half-lives tended to follow a distribution equivalent to the power distribution in the reactor core. Second, the shortest-lived groups of DNPs decayed almost entirely before reentering the core, whereas a significant fraction of the long-lived groups of DNPs reentered the reactor core.

When comparing the distribution of DNPs across different group representations, it was shown that using fewer groups resulted in a distribution shifted toward the upper edge of the core. As a result, a significant fraction of the DNPs is expected to be simulated removed from the core. Depending on their half-lives, a fraction of these DNPs may not decay in the loop and renter the core. This fraction depends on the fuel salt transit time in the loop (τ_L), with more DNPs decaying or reentering the core based on their half-lives. Therefore, reduced DNPs models cannot accurately

represent the distribution of DNPs in the core. Increasing the number of groups improves the accuracy of both the simulated spatial distribution and decay location of these precursors.

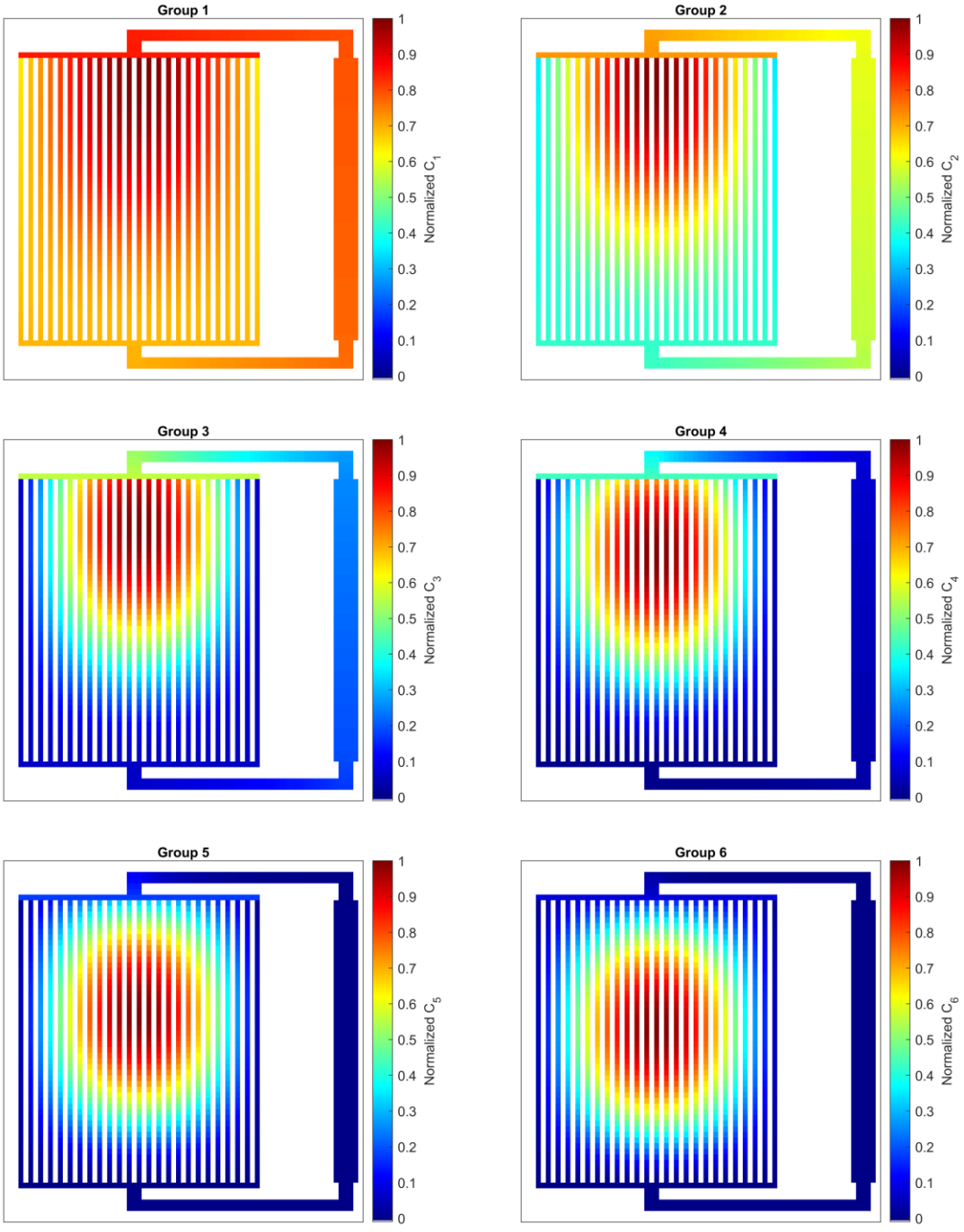

Figure 10. Normalized concentration of DNPs in the primary loop using the 6-group model.

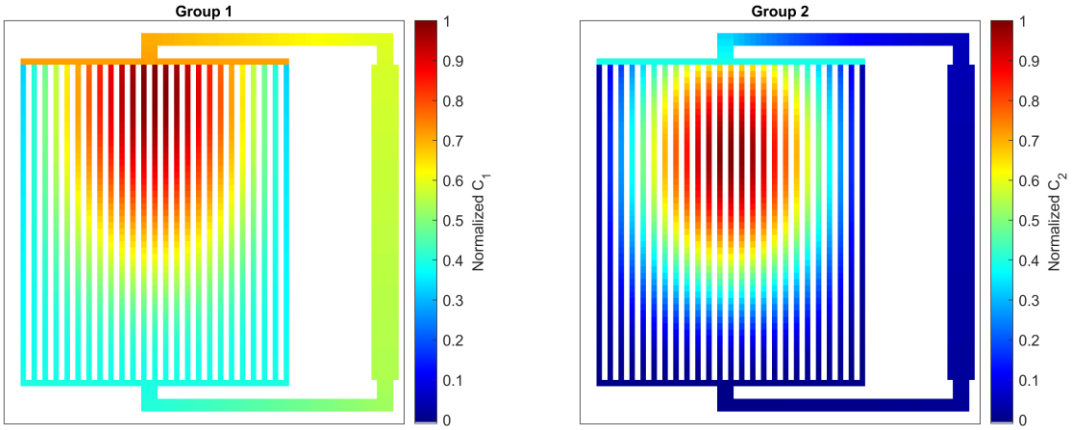

Figure 11. Normalized concentration of DNPs in the primary loop using the 2-group model.

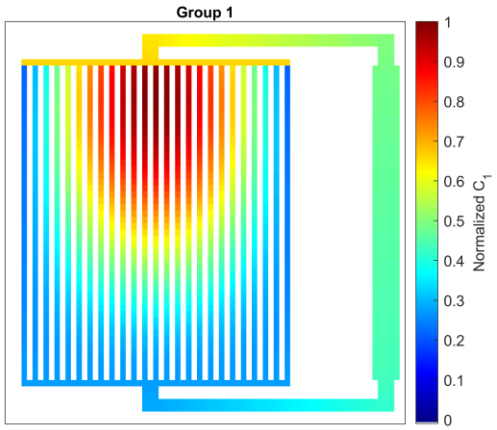

Figure 12. Normalized concentration of DNPs in the primary loop using the 1-group model.

In MSRs, a fraction of DNPs leave the core with the flowing fuel salt. While some of these DNPs may later reenter the core, their temporary removal affects the delayed neutron population within the core. Thus, the core net reactivity is a non-zero value. This positive reactivity has to compensate for the reactivity loss because of the removal of delayed neutrons due to DNPs being removed during the fuel salt circulation. The percentage of DNPs removed from each group and the reactivity loss using different DNPs models are summarized in

Table 1, Table 2, and Table 3.

Using the six-group model, it can be demonstrated that groups with the longest half-lives had a significant fraction of their precursors removed from the core. In contrast, groups with the shortest half-lives had only a tiny fraction removed. The fraction of precursors removed depends on their spatial distribution within the core, which is influenced by the fuel salt flow and the decay characteristics of each group. The reactivity loss value did not follow this trend, as different groups have varying abundances (delayed neutron fractions) and half-lives. Although the group with the longest half-life, group 1, had a significant fraction of its precursors removed due to the shifted distribution, its contribution to reactivity loss was not the highest. This can be explained by its lower delayed neutron fraction and the longer half-live, which allowed a significant fraction of the precursors to renter the core. Group 2, however, contributed the most to the reactivity loss. This is due to the significant fraction of its precursors being removed from the core, its shorter half-life, and its higher delayed neutron fraction.

When comparing the percentage of DNPs removed from each group and the reactivity loss values across different models, it becomes evident that reduced models resulted in a lack of accurate representation of the distribution of DNPs and, thus, the reactivity loss estimates. In this reactor design, the reactivity loss value was shown to be lower using more detailed group representations. These models better capture the nuances of precursor distribution and decay, resulting in more precise reactor reactivity loss predictions. Compared to the experimental reactivity loss value of 100.5 pcm reported for the MSRE (Abuqudaira et al., 2024), more detailed models with more groups provided more accurate estimates of reactivity loss.

Table 1. The percentage of DNPs removed from each group and the reactivity loss using the 6-group DNPs model.

Group	Percentage of DNPs removed from the core	Reactivity loss (pcm)
1	65.82%	15.01
2	64.91%	51.15
3	52.86%	35.10
4	30.01%	22.08
5	5.24%	0.71
6	1.30%	0.11
Total	47.03%	124.17

Table 2. The percentage of DNPs removed from each group and the reactivity loss using the 2-group DNPs model.

Group	Percentage of DNPs removed from the core	Reactivity loss (pcm)
1	64.75%	108.77
2	24.27%	23.30
Total	50.03%	132.07

Table 3. The percentage of DNPs removed from each group and the reactivity loss using the 1-group DNPs model.

Group	Percentage of DNPs removed from the core	Reactivity loss (pcm)
1	63.38%	167.32

4.1.2. Transients

Two transient events were simulated using reduced and conventional DNPs models. The first transient involved a step reactivity insertion simulation. In the second transient, a primary pump failure resulting in a loss of flow rate was simulated.

4.1.2.1 Reactivity Insertion

In this transient event, a positive reactivity of $0.1\beta_{eff}$ was inserted following steady-state reactor operation. As a result, the reactor power and fuel salt temperature started to increase. The increase in fuel salt temperature triggered negative reactivity feedback. Eventually, the negative reactivity feedback counteracted the inserted positive reactivity, and reactor power started to decrease. A plateau in the reactor power was observed due to the "hot" fuel salt exiting the core and "cold" fuel salt entering the core, which introduced a positive reactivity feedback, balancing the negative reactivity feedback due to the temperature increase. Eventually, the negative reactivity feedback reduced reactor power with minor oscillations due to the positive/negative reactivity feedback because of the fuel salt circulation process. Such a general trend was observed regardless of the model of DNPs implemented in the simulation. The reactor power using different models of DNPs and the relative deviation in reactor power using reduced DNPs models from the 6-group model following a step reactivity insertion of $0.1\beta_{eff}$ is shown in Figure 13.

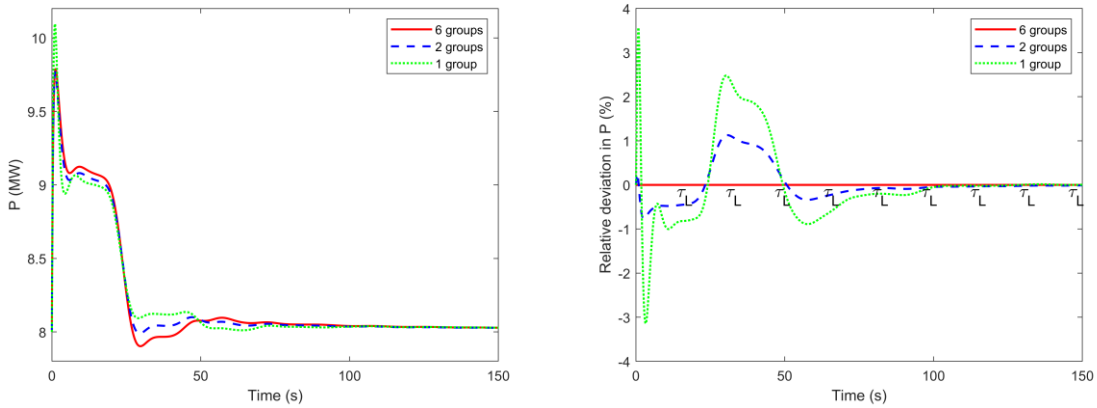

Figure 13. Reactor power using different DNPs models and the relative deviation in power estimates using reduced DNPs models from the 6-group model following a step reactivity insertion of $0.1\beta_{eff}$.

It can be observed that the deviation from the reference 6-groups model decreased as the number of groups increased. In addition, the deviation in the estimated power is more pronounced during the power peak. Using fewer groups resulted in the overestimation of the power peak value. In addition, it resulted in an underestimation of the time to reach the peak. Following the power decrease, reduced models started to fluctuate compared with the 6-groups model due to the simulated reactivity feedback relative to the reactivity loss value. These fluctuations were particularly pronounced following time intervals of approximately (τ_L), corresponding to the fuel salt transit time in the loop outside the core. The periodic markers (τ_L) on the time axis represent the fuel salt transit time outside the core, highlighting its influence on reactivity fluctuations. The magnitude of these fluctuations varied between models based on the fraction of DNPs reentering the core, highlighting how each model estimated the fraction of DNPs reentering the core after circulation through the external loop. However, as time progressed, the deviations gradually decreased as the reactor approached a new equilibrium, eventually becoming negligible once the system stabilized.

The reactivity loss following the reactivity insertion as a function of time and the relative deviation using reduced DNPs models from the 6-group model is shown in Figure 14. The reactivity insertion resulted in a rapid increase in reactor power and, thus, the production of DNPs. More DNPs were removed from the core, and the reactivity loss increased. The negative reactivity feedback due to the fuel salt temperature increase counteracted the external reactivity insertion, as shown in Figure 15. Eventually, the reactivity loss stabilized at a value corresponding to the new simulated power level. The same behavior was observed regardless of the use of different DNPs models. The deviation in the simulated average fuel salt temperature in the reduced models compared to the 6-group model was small. However, the high deviation in the reactivity loss estimates affected the simulated reactivity feedback and, thus, the power behavior over time.

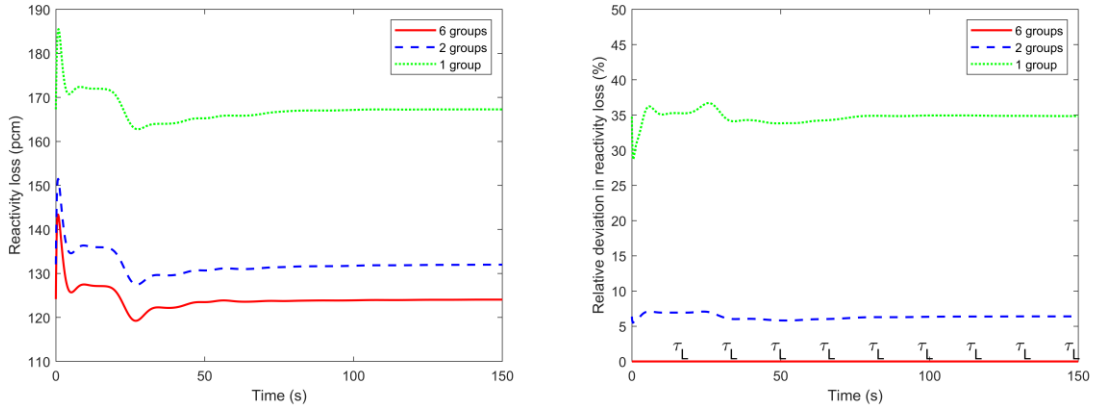

Figure 14. Reactivity loss using different DNPs models and the relative deviation in reactivity loss estimates using reduced DNPs models from the 6-group model following a step reactivity insertion of $0.1\beta_{eff}$.

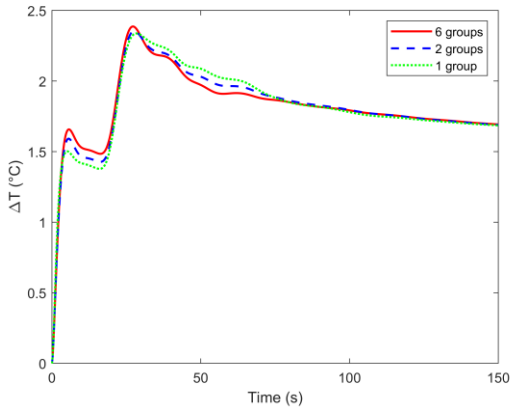

Figure 15. Average fuel salt temperature change using different DNPs models following a step reactivity insertion of $0.1\beta_{eff}$.

To summarize the observations in reactivity insertion transient of $0.1\beta_{eff}$, although the reduced models preserved the overall power behavior, they introduced inaccuracies in key transient characteristics, including the peak power estimate and the power evolution over time. The use of reduced DNPs models led to overestimating the power peak compared to the conventional 6-group model. Specifically, the 1-group model overestimated the peak power by approximately 3.5%, while the 2-group model resulted in a deviation of only 0.25%. The discrepancies in reactivity loss estimates contributed to fluctuations in power deviation over time.

4.1.2.2 Pump Failure

In this transient, a simulation of a primary pump failure was carried out. As a result of the pump failure, the mass flow rate of the fuel salt in the primary loop started to decrease exponentially. Eventually, the mass flow rate was reduced by 25%. The normalized mass flow rate of the fuel salt in the primary loop following this pump failure is shown in Figure 16. The reduction in the mass flow rate caused an increase in the fuel salt temperature, which induced a negative reactivity feedback, acting in favor of a power decrease. This negative reactivity feedback

exceeded the excess reactivity introduced by the reduced loss of DNPs at the lower mass flow rate. The change in reactor power and the relative deviation in reactor power using reduced DNPs models from the 6-group model, reactivity loss and the relative deviation in reactivity loss using reduced DNPs models from the 6-group model, and average fuel salt temperature using different group representations of DNPs following the primary pump failure are shown in Figure 17, Figure 18, and Figure 19.

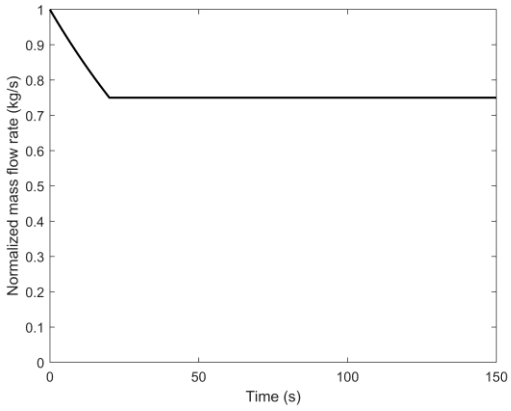

Figure 16. Normalized fuel salt mass flow rate in the primary loop following a primary pump failure.

As the mass flow rate decreased, the removal rate of DNPs also decreased, leading to a lower reactivity loss value. However, the removal rates of individual precursor groups varied depending on the DNPs model used. Thus, the change in the reactivity loss value is not the same for all models. The change in the estimated reactivity loss as a function of the mass flow rate in the loop is summarized in Table 4. It can be observed that the reactivity loss value changed most significantly using the 6-group model. Therefore, compared with the 6-group model, the power dip value was overestimated using the 1-group and 2-group DNPs models.

Following the power dip, the decrease in fuel salt temperature led to negative reactivity feedback, which resulted in a power increase, reaching a peak. At this peak, the power deviation

using the reduced models from the 6-group model is maximum, where it was around 3% using the 1-group model and slightly above 1% using the 1-group model. Mainly, this behavior is due to increased reactivity loss deviation from the 6-group model. The reactor power showed oscillations caused by the reactivity feedback caused by the fuel salt circulation in the primary loop. These oscillations gradually decreased, and the system approached a stable state with a new reactivity loss value.

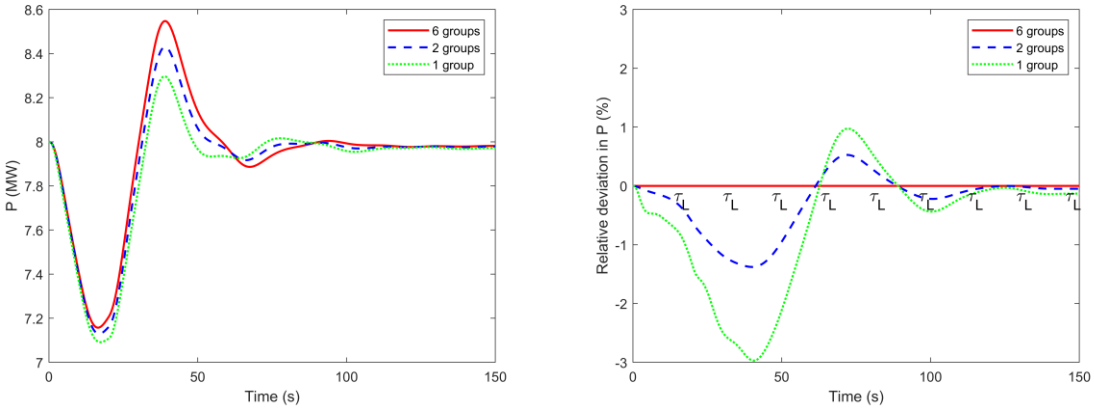

Figure 17. Reactor power using different DNPs models and the relative deviation in power estimates using reduced DNPs models from the 6-group model following a primary loop pump failure.

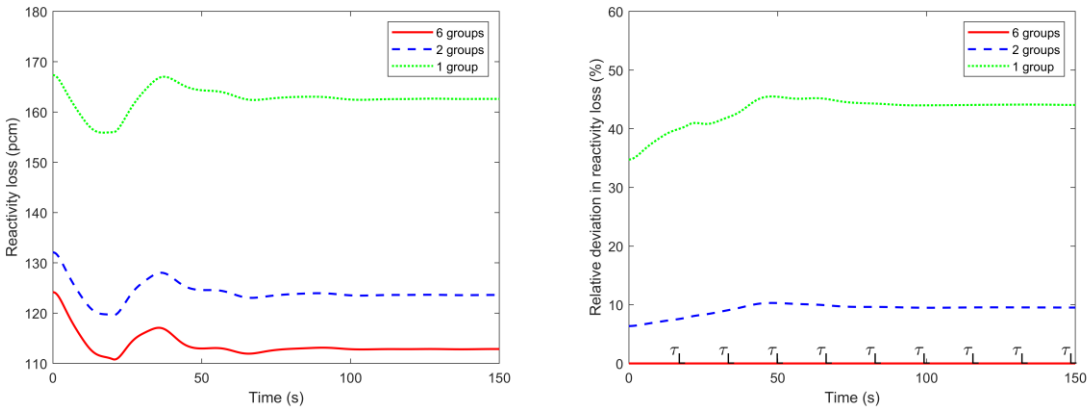

Figure 18. Reactivity loss using different DNPs models and the relative deviation in reactivity loss estimates using reduced DNPs models from the 6-group model following a primary loop pump failure.

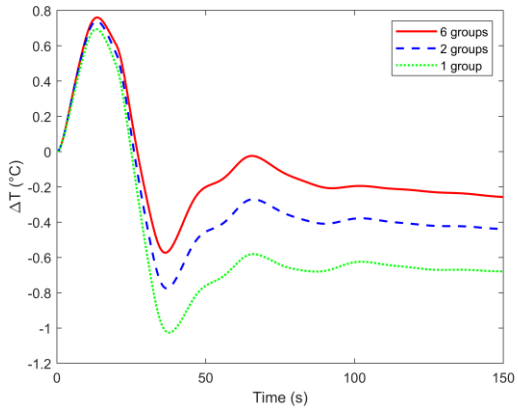

Figure 19. Average fuel salt temperature change using different DNPs models following a primary loop pump failure.

Table 4. Reactivity loss as a function of the mass flow rate in the primary loop using different DNPs models.

Number of groups	Reactivity loss (pcm)		Change (%)
	100% flow rate	75% flow rate	
1	167.32	162.60	-2.82
2	132.08	123.62	-6.41
6	124.17	112.87	-9.10

To summarize, the DNPs model influenced the simulated removal rate of DNPs, affecting the reactivity loss estimates. During a pump failure transient, the change in reactivity loss value was different, resulting in further deviation in the estimated reactivity loss in the reduced models from the conventional 6-group model. The average fuel salt temperature deviation in the reduced models, compared to the 6-group model, was significantly greater than that observed in the reactivity insertion transient. These differences impacted the simulated transient behavior, including the magnitude of the initial power dip and subsequent oscillations.

4.2. Expanded DNPs Models

Additional simulations incorporating expanded DNPs representations were performed to enable comparative analysis and assess the influence of the increased number of groups of DNPs on their simulated distribution, reactivity loss, and the reactor dynamic response.

4.2.1. Steady-State

The distribution of DNPs in the primary loop using the 6-group model is similar to what was shown in Figure 10. For the 7-group and 8-group models, the normalized concentration of DNPs groups is shown in Figure 20 and Figure 21. Expanded DNPs models led to a more accurate representation of the DNPs concentration in the primary loop. Specifically, group 2 in the 6-group model was expanded into two separate groups in the 7-group model, and the seventh group in the 7-group model was further expanded into two groups in the 8-group model. The impact of this expansion on reactivity loss depends on how the altered distribution of DNPs, combined with the half-life of the expanded groups, influences the removal and reentry of DNPs into the core. The fraction of DNPs reentering the core is reactor design-dependent, influenced by the fuel salt transit time outside the core (τ_L). The percentage of DNPs removed from the core and the reactivity loss values are summarized in Table 5, Table 6, and Table 7.

The overall observations align with findings from the reduced models, where groups with the longest half-lives exhibited a distribution shifted toward the upper region of the core, leading to significant removal from the core. However, a substantial fraction of these precursors managed to reenter the core due to their long half-lives relative to the fuel transit time outside the core in this design ($\tau_L \approx 16.5$ seconds). In contrast, the distribution of groups with the shortest half-lives remained more aligned with the power distribution in the core, resulting in minimal removal.

Additionally, only a tiny fraction of these short-lived precursors reentered the core, as their half-lives were much shorter than τ_L, leading to their decay before completing the loop.

Therefore, the reactivity loss value decreased by expanding group 2 in the 6-group model into groups 3 and 4 in the 7-group model. This can be explained by the redistribution of DNPs, where the newly defined groups captured a more refined decay behavior. This shift resulted in a lower overall removal fraction and increased the fraction of DNPs that reentered the core before decaying, thereby reducing the net reactivity loss. Conversely, the reactivity loss value increased when group 7 in the 7-group model was expanded into groups 7 and 8 in the 8-group model. This increase can be attributed to the redistribution of DNPs, where the newly introduced group captured a portion of precursors with an even longer half-life. As a result, more precursors were transported out of the core before decaying, increasing the overall reactivity loss. However, the difference in estimated reactivity loss between the 6-group, 7-group, and 8-group models was minimal, not exceeding 0.08%. Thus, while the reduced models exhibited a significant deviation from the 6-group model in terms of reactivity loss, the expanded models, despite offering a more detailed distribution of DNPs in the primary loop of an MSR, resulted in only a negligible difference in the estimated reactivity loss.

514

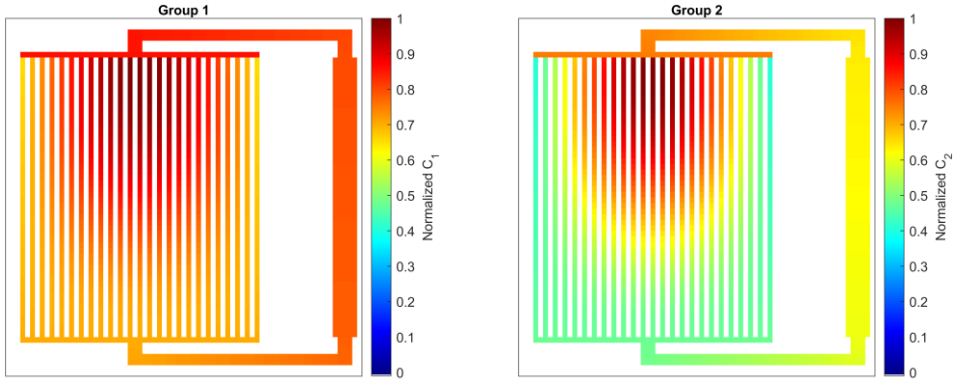

515

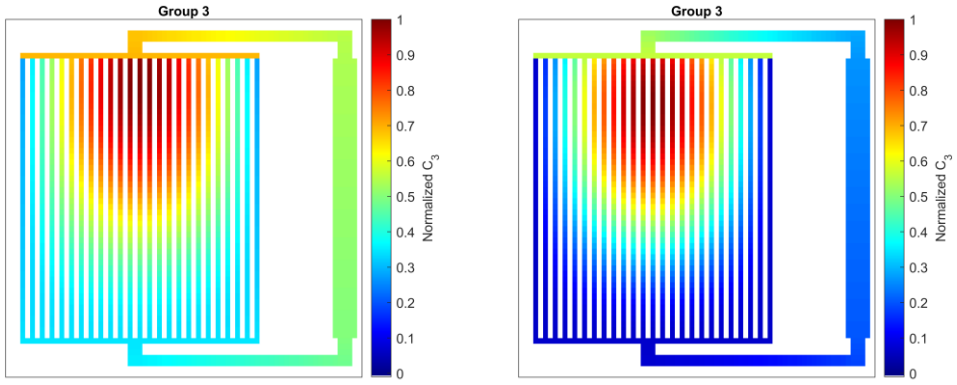

516

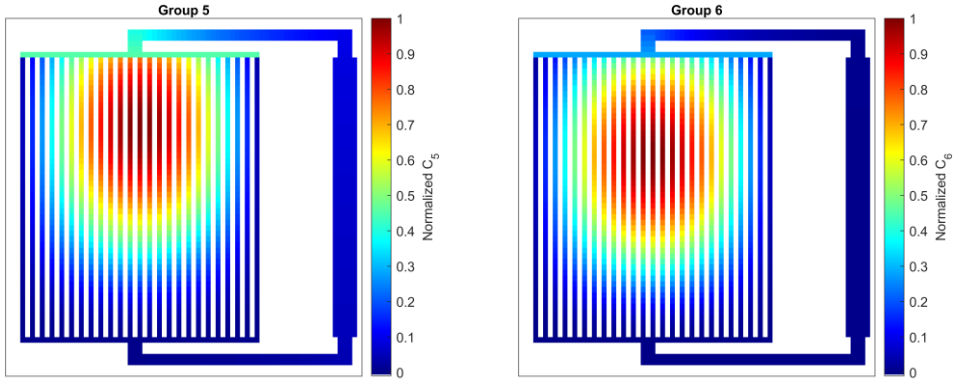

517

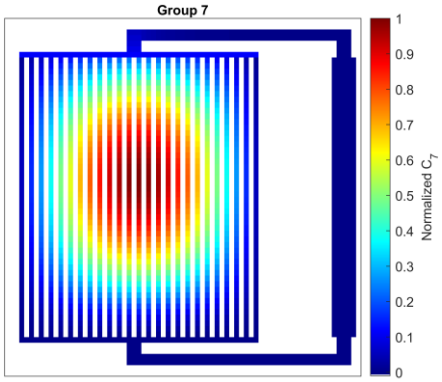

518 Figure 20. Normalized concentration of DNPs in the primary loop using the 7-group model.

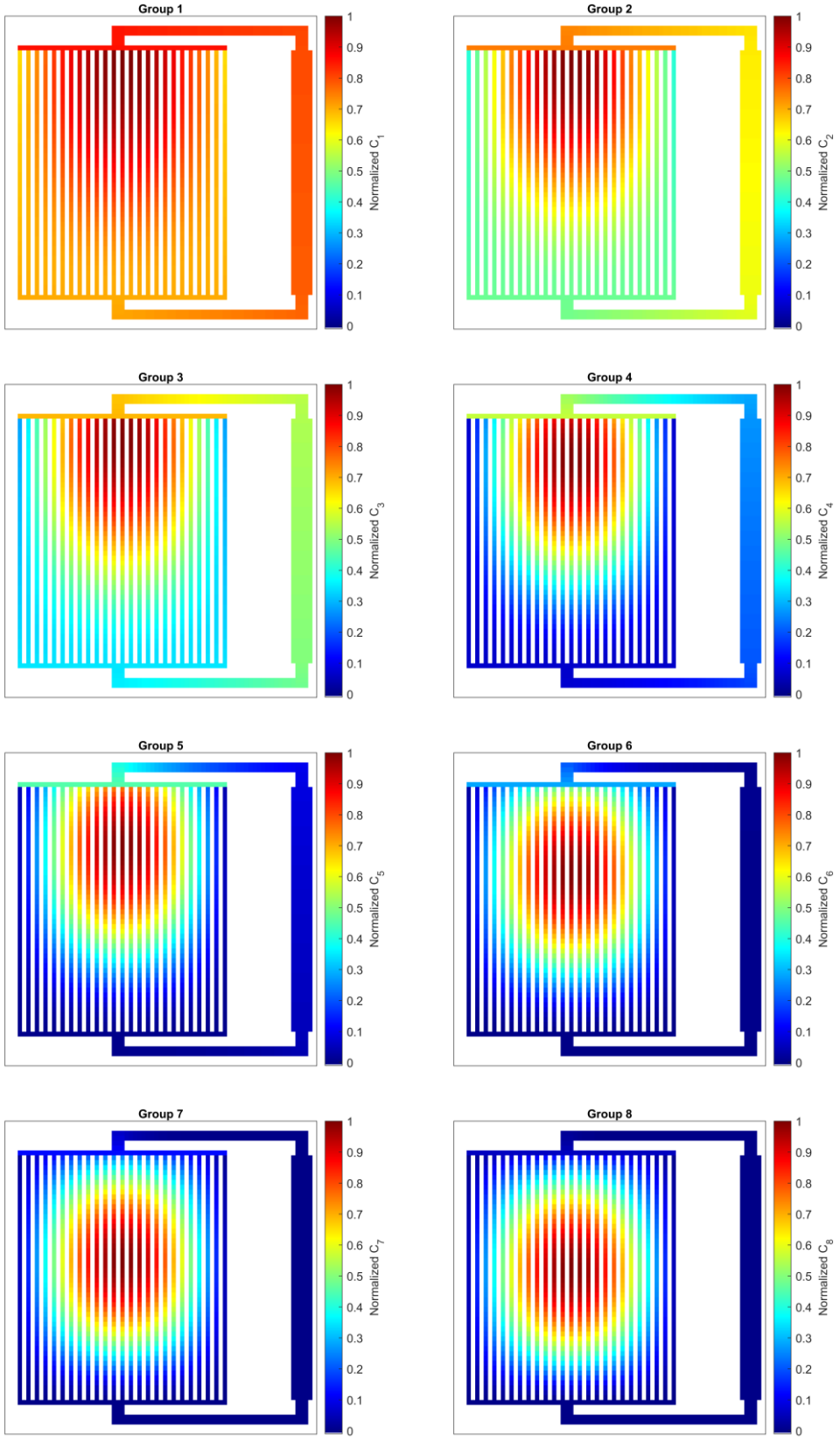

Figure 21. Normalized concentration of DNPs in the primary loop using the 8-group model.

524 Table 5. The percentage of DNPs removed from the core and the reactivity loss using the 6-group DNPs model.

Group	Percentage of DNPs removed from the core	Reactivity loss (pcm)
1	65.84%	13.85
2	65.23%	54.31
3	64.29%	28.36
4	53.72%	26.12
5	33.20%	1.26
6	12.26%	0.41
Total	47.09%	124.31

525

526

527 Table 6. The percentage of DNPs removed from each group and the reactivity loss using the 7-group DNPs model.

Group	Percentage of DNPs removed from the core	Reactivity loss (pcm)
1	65.84%	13.85
2	65.23%	28.76
3	64.29%	25.46
4	53.72%	28.36
5	33.20%	26.12
6	12.26%	1.26
7	2.35%	0.41
Total	47.05%	124.22

528

529

530

531

532

Table 7. The percentage of DNPs removed from each group and the reactivity loss using the 8-group DNPs model.

Group	Percentage of DNPs removed from the core	Reactivity loss (pcm)
1	65.84%	13.85
2	65.23%	28.76
3	64.29%	25.46
4	53.72%	28.36
5	33.20%	26.12
6	12.26%	1.26
7	2.75%	0.41
8	0.70%	0.02
Total	47.06%	124.24

4.2.2. Transients

SDAT was used to simulate two transient events implementing the expanded and 6-group models. The first transient involved a step reactivity insertion simulation, while the second transient simulated a primary pump failure.

4.2.2.1 Reactivity Insertion

In this transient, a step reactivity insertion of $0.1\beta_{eff}$ produced the same physical phenomena observed in the reduced models' section. However, the deviation in reactor power predicted by the expanded DNPs models, compared to the conventional 6-group model, was negligible. Figure 22 illustrates the reactor power for different DNPs models and the relative deviation of expanded DNPs models from the 6-group model following the reactivity insertion. The deviation in estimating the time to reach the peak and the power peak value was minimal compared to the reduced models. The 8-group model slightly overestimated the power peak, while the 7-group

model underestimated it compared to the 6-group model. The maximum relative deviation in reactor power following the reactivity insertion was limited to 0.03%, which was achieved after two fuel salt transit times outside the core ($2\tau_L$). Subsequently, the deviation of the expanded models from the conventional 6-group model gradually decreased over time.

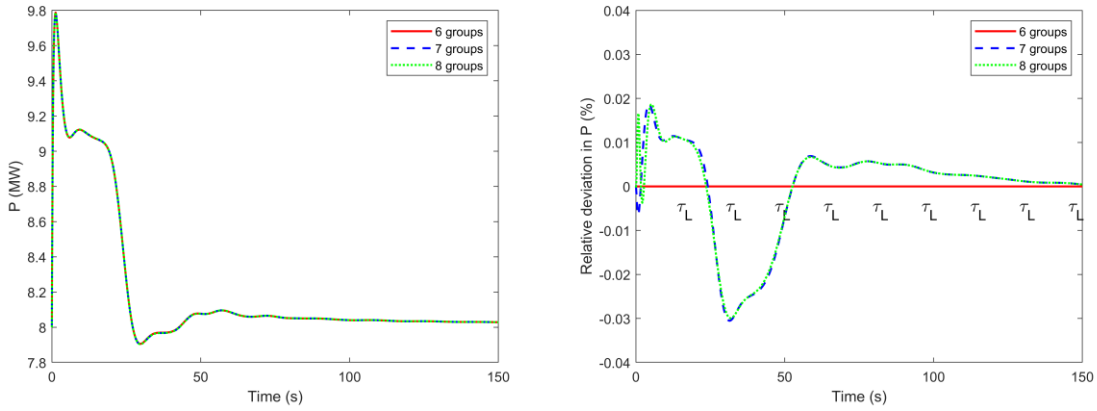

Figure 22. Reactor power using different DNPs models and the relative deviation in power estimates of expanded DNPs models from the 6-group model following a step reactivity insertion of $0.1\beta_{eff}$.

Figure 23 shows that the reactivity loss value estimated by the expanded models was underestimated compared to the conventional 6-group model. Fluctuations in the reactivity loss estimates by the expanded models, compared to the 6-group model, were observed due to fuel salt circulation. Fluctuations in the reactivity loss estimates in the expanded models compared to the 6-group model introduced reactivity feedback fluctuations. However, the deviation in the temperature change was minimal, as shown in Figure 24.

To summarize this transient, while the use of expanded DNPs resulted in a more accurate representation of the DNPs distribution in the primary loop, the estimated reactivity loss remained close to that of the conventional 6-group model, leading to minimal deviation in the reactor's response to reactivity insertion transient of $0.1\beta_{eff}$. Additional simulations of transients involving reactivity insertions up to β_{eff} were conducted. A similar behavior was observed, with minimal

deviation between the expanded and 6-group models. Thus, the expanded models' impact on the reactor's dynamic response to reactivity insertion transients was negligible, suggesting that the additional groups may not significantly improve transient behavior within the studied reactivity range.

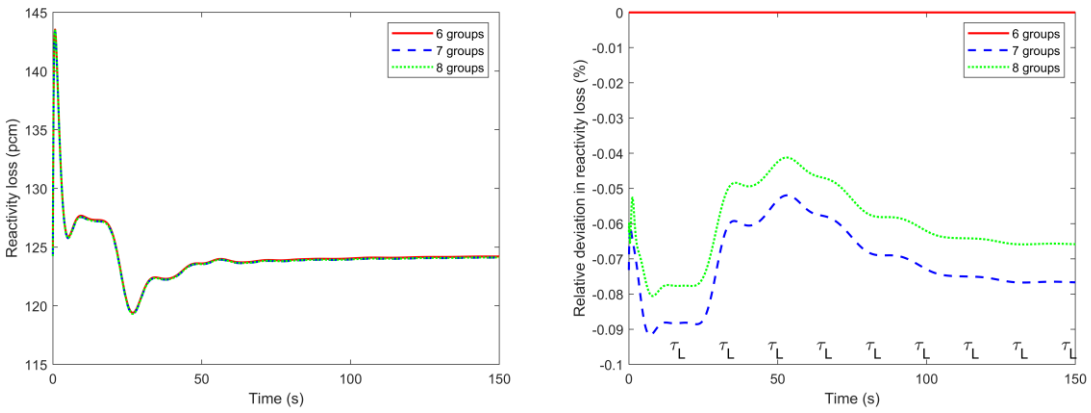

Figure 23. Reactivity loss using different DNPs models and the relative deviation in reactivity loss estimates of expanded models from the 6-group model following a step reactivity insertion of $0.1\beta_{eff}$.

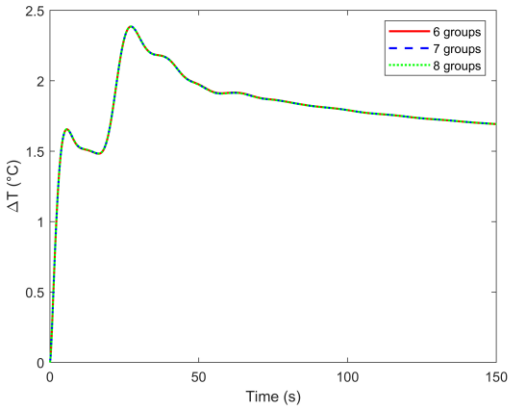

Figure 24. Average fuel salt temperature change using different DNPs models following a step reactivity insertion of $0.1\beta_{eff}$.

4.2.2.2 Pump Failure

The reactor power following the primary pump failure and the relative deviation in reactor power using expanded DNPs models from the 6-group model is shown in Figure 25. The reactor

power evolution remained consistent across different DNPs models following the pump failure. This consistency is a result of the slight deviation in the reactivity loss estimates over time using the expanded and conventional 6-group model. The reactivity loss and the relative deviation in reactivity loss estimates using expanded DNPs models from the 6-group model following a primary loop pump failure are shown in Figure 26. While the removal rate of DNPs from the core decreased as the mass flow rate decreased, this decrease was almost identical in the 6-group, 7-group, and 8-group models, as summarized in Table 8. Consequently, the deviation in reactivity loss was minimal, and the simulated average fuel salt temperature exhibited negligible differences across all DNPs models, as shown in Figure 27.

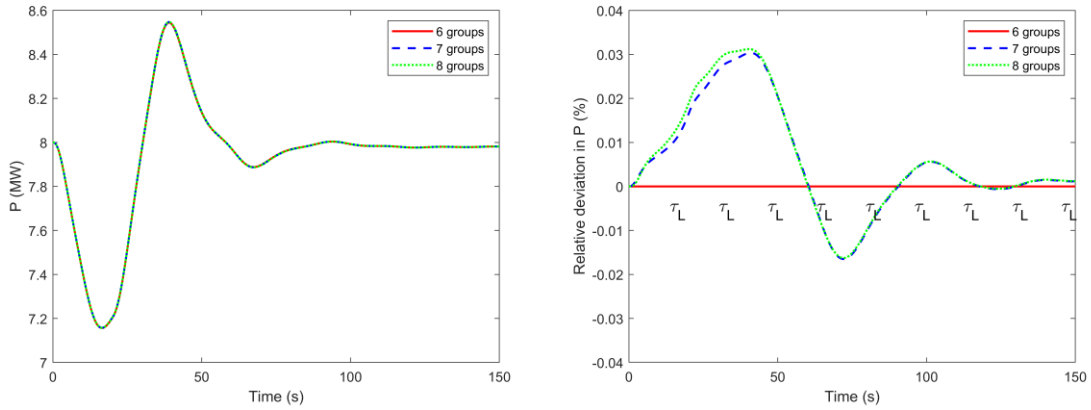

Figure 25. Reactor power using different DNPs models and the relative deviation in reactor power using expanded DNPs models from the 6-group model following a primary pump failure.

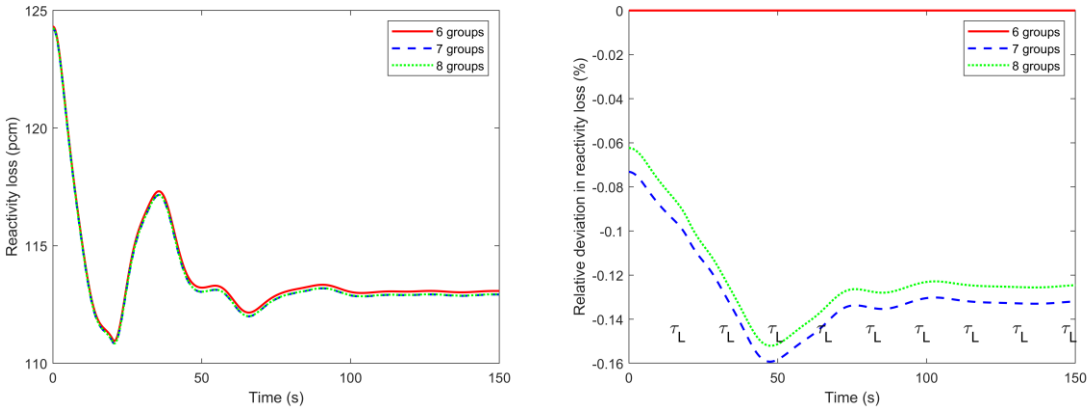

Figure 26. Reactivity loss using different DNPs models and the relative deviation in reactivity loss estimates using expanded DNPs models from the 6-group model following a primary loop pump failure.

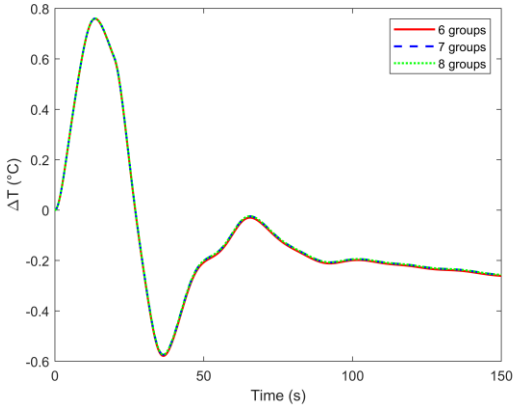

Figure 27. Average fuel salt temperature change using different DNPs models following a primary pump failure.

Table 8. Reactivity loss as a function of the mass flow rate in the primary loop using different DNPs models.

Number of groups	Reactivity loss (pcm)		Change (%)
	100% flow rate	75% flow rate	
6	124.31	113.07	-9.04%
7	124.22	112.93	-9.09%
8	124.24	112.93	-9.10%

To summarize, the change in reactivity loss as the mass flow rate decreased was comparable between the expanded and conventional models. This indicates that while the expanded models offered a more detailed distribution, the removal rate and reactivity loss estimates from the expanded models were found to be in close agreement with those from the 6-group model. As a result, the maximum deviation in reactor power was limited to just 0.03% when using the 8-group model compared to the 6-group model, highlighting the minimal impact of the expanded model on overall power predictions in a pump failure transient simulation.

4.3. Prospective Trend

As demonstrated in previous subsections, increasing the number of groups of DNPs improved the representation of their simulated distribution and allowed for more precise tracking of their behavior. In the reduced models, a higher number of groups decreased the percentage of DNPs removed from the core, thereby reducing the reactivity loss. Similarly, in the expanded models, this trend was observed except for the 7-group and 8-group cases, where an increase in the number of groups resulted in a higher percentage of DNPs removed from the core and, consequently, a greater reactivity loss. The reactivity loss values using SDAT simulations are compared with the reported experimental value, as shown in Table 9. These findings underscored the impact of the number of groups of DNPs on the accuracy of their simulated removal from the core and the corresponding reactivity loss.

Table 9. Reactivity loss values compared to the experimental result.

Method	Number of groups of DNPs	Reactivity loss (pcm)
SDAT – Reduced representations	1	167.32
	2	132.07
	6	124.17
SDAT – Expanded representations	6	124.31
	7	124.22
	8	124.24
Experimental	-	100.5

These reactivity loss values were used to extrapolate the required number of groups to achieve a reactivity loss value identical to the experimental one of 100.5 pcm. The reactivity loss values obtained from reduced models were fitted using various mathematical approaches, with power-law fitting yielding the best fit. Extrapolation using the power fit determined that at least 17 groups of DNPs are necessary to reproduce the experimentally observed reactivity loss value. Fitting the combined data from reduced and expanded models indicated that approximately 30 groups of DNPs would be required to converge to the experimental result. Extrapolation of the reactivity loss values to obtain the required number of groups of DNPs needed to match the experimental reactivity loss value is shown in Figure 28.

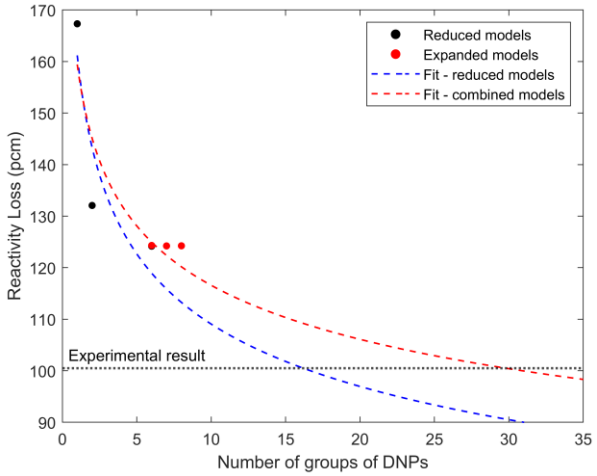

Figure 28. Number of groups of DNPs for matching the experimental reactivity loss value of 100.5 pcm.

However, several sources of errors can be considered in these estimations:

- The power-law fit used to extrapolate the required number of groups is subject to inherent uncertainties. The fitting process depends on the dataset used, and extrapolations beyond the available data points introduce potential deviations. Moreover, the reactivity loss values obtained may not always follow a strict power-law trend, leading to additional uncertainty in determining the required number of groups.
- SDAT employs a one-dimensional multi-channel treatment of DNPs, which introduces approximations that may not fully capture their drift and diffusion in three-dimensional reactor geometries. These simplifications can lead to discrepancies in the simulated distribution, affecting the estimation of reactivity loss.
- The experimental measurement of the reactivity loss value has its own uncertainties. Additionally, several published articles have raised concerns about the accuracy of the reported results from MSRE tests (Mochizuki, 2022; Zanetti et al., 2015).

- The use of the extended model with 8-group data does not include importance functions, relying solely on the physical delayed neutron fractions rather than the effective values. This limitation introduces a source of error in the fitting process when using combined models.

Despite these sources of error, the results still indicate a potential trend in the relationship between the number of groups of DNPs and the simulated reactivity loss value. However, while increasing the number of groups improves the accuracy of the precursors' distribution and enhances fidelity in tracking precursors, it has minimal impact on the reactor's dynamic response to transients.

5. Conclusions

This study assessed the impact of the adopted delayed neutron precursors (DNPs) model on molten salt reactor dynamics simulations. The distribution of DNPs in the primary loop, the removal percentage of DNPs, and the reactivity loss during steady-state reactor operation were compared using reduced and expanded DNPs models. Additionally, the simulated reactor power following initiated transients using reduced and expanded models was analyzed, all using the System Dynamics Analysis Tool (SDAT). Reduced models were obtained by condensing a 6-group model into 2-group and 1-group models. An extended 8-group model was used to derive condensed 7-group and 6-group models.

Results showed that adopting reduced DNPs models led to a misrepresentation of the actual DNPs distribution in the primary loop. Due to the fuel salt circulation, these reduced models shifted the simulated DNPs distributions toward the upper part of the core. As a result, a higher fraction of DNPs was removed from the core than the actual fraction. Depending on the design

configuration, this removed fraction may either reenter the core or decay outside, depending on the decay characteristics of the individual groups. Therefore, this could lead to either overestimating or underestimating the reactivity loss value. For the Molten Salt Reactor Experiment (MSRE) design, the reactivity loss value was overestimated using the reduced models compared to the conventional 6-group model. This deviation in the estimated reactivity loss resulted in an overestimation of the power increase in a reactivity insertion of $0.1\beta_{eff}$ and an overestimation of the power decrease in primary pump failure transient simulations. This deviation in the estimated reactivity loss resulted in oscillatory behavior of the power deviation from the 6-group model due to the continuous fuel salt movement.

Using expanded models of DNPs resulted in a more detailed representation of the DNPs in the primary loop and underestimating the reactivity loss value compared to the 6-group model. However, the influence of this distribution on the removal percentage and reactivity loss estimates was negligible. Furthermore, the deviation in simulated power following a reactivity insertion and pump failure transients was minimal. These findings suggest that expanded models improve the fidelity of DNPs distribution modeling. However, their impact on key reactor dynamics parameters, such as reactivity loss and power response, remains limited compared to the 6-group model.

The fitting of the obtained reactivity loss data demonstrated that increasing the number of groups could help match the experimental reactivity loss value observed in the MSRE. Extrapolation indicated that at least 17 groups are necessary when using reduced models. Combining data from reduced and expanded models suggested that approximately 30 groups would be required to converge to the experimental result. However, several sources of error introduce potential deviations to these estimates. Despite these uncertainties, the results highlight

a trend in the relationship between the number of groups and simulated reactivity loss. Nevertheless, while increasing the number of groups enhances the fidelity of precursor tracking, it has minimal impact on the reactor's overall dynamic response to transients.

Future research should focus on examining the impact of uncertainties in DNPs group fractions on the distribution of precursors, reactivity loss, and the reactor's dynamic response. In addition, a comprehensive study on the influence of delayed neutron data from different nuclear data libraries on key reactor kinetics parameters is necessary. Investigating these aspects will enhance the accuracy of reactor simulations and improve confidence in transient analysis for MSRs and other advanced reactor systems.

6. References

Abram, T., Ion, S., 2008. Generation-IV nuclear power: A review of the state of the science. Energy Policy 36, 4323–4330. https://doi.org/10.1016/j.enpol.2008.09.059

Abuqudaira, T., Tsvetkov, P., Sabharwall, P., 2024. Dynamics of Molten Salt Reactor with Operating Heaters. Nuclear Science and Engineering 1–22. https://doi.org/10.1080/00295639.2024.2423132

Abuqudaira, T., Tsvetkov, P., Sabharwall, P., 2023. Perspective Chapter: Assessment of Nuclear Sensors and Instrumentation Maturity in Advanced Nuclear Reactors, in: Nuclear Fission - From Fundamentals to Applications. https://doi.org/10.5772/intechopen.113403

Brady, M.C., 1989. Evaluation and Application of Delayed Neutron Precursor Data. United States. https://doi.org/10.2172/6187550

Brown, N.R., Diamond, D.J., Bajorek, S., Denning, R., 2020. Thermal-Hydraulic and Neutronic Phenomena Important in Modeling and Simulation of Liquid-Fuel Molten Salt Reactors. Nucl Technol 206, 322–338. https://doi.org/10.1080/00295450.2019.1590077

Cammi, A., Fiorina, C., Guerrieri, C., Luzzi, L., 2012. Dimensional effects in the modelling of MSR dynamics: Moving on from simplified schemes of analysis to a multi-physics modelling approach, in: Nuclear Engineering and Design. pp. 12–26. https://doi.org/10.1016/j.nucengdes.2011.08.002

Duderstadt, J.J., Hamilton, L.J., 1976. Nuclear Reactor Analysis. Wiley.

Elsheikh, B.M., 2013. Safety assessment of molten salt reactors in comparison with light water reactors. J Radiat Res Appl Sci 6, 63–70. https://doi.org/10.1016/j.jrras.2013.10.008

Hetrick, D.L., 1971. Dynamics of Nuclear Reactors. University of Chicago Press.

Huff, K.D., 2019. Identifying MSR Multiphysics Modeling Challenges.

Jo, Y., Lee, H.-S., Lee, E.-K., 2022. Investigation of Impact of Delayed Neutron Data on Dynamic Reactivity, Transactions of the Korean Nuclear Society Autumn Meeting Changwon.

Keepin, G.R., 1965. Physics of Nuclear Kinetics, 1st ed. Addison-Wesley Publishing Company.

Kerlin T. W., Ball S. J., Steffy R. C., 1971. Theoretical Dynamics Analysis of the Molten-Salt Reactor Experiment. Nucl Technol 10, 118–132. https://doi.org/10.13182/nt71-a30920

Krepel, J., Rohde, U., Grundmann, U., Weiss, F.P., 2008. Dynamics of molten salt reactors, in: Nuclear Technology. American Nuclear Society, pp. 34–44. https://doi.org/10.13182/NT08-A4006

LeBlanc, D., 2010. Molten salt reactors: A new beginning for an old idea. Nuclear Engineering and Design 240, 1644–1656. https://doi.org/10.1016/j.nucengdes.2009.12.033

Leconte, P., Belverge, D., Bernard, D., Chebboubi, A., Kessedjian, G., Foligno, D., Geslot, B., Sardet, A., Casoli, P., Kooyman, T., Pépino, A., Domergue, C., Doré, D., Ledoux, X., Mathieu, L., Méplan, O., Billebaud, A., Cheymol, B., Marie, N., Lecolley, F.R., Lecouey, J.L., Koester, U., Solder, T., Mutti, P., 2024. Accurate measurements of delayed neutron data for reactor applications: methodology and application to 235U(nth,f). European Physical Journal A 60. https://doi.org/10.1140/epja/s10050-024-01402-7

Macphee, J., 1958. The Kinetics of Circulating Fuel Reactors. Nuclear Science and Engineering 4, 588–597. https://doi.org/10.13182/nse4-588-597

McIntyre, P., Assadi, S., Badgley, K., Baker, W., Comeaux, J., Gerity, J., Kellams, J., McInturff, A., Pogue, N., Phongikaroon, S., Sattarov, A., Simpson, M., Sooby, E., Tsvetkov, P., 2013. Accelerator-driven subcritical fission in molten salt core: Closing the nuclear fuel cycle for green nuclear energy, in: AIP Conference Proceedings. pp. 636–642. https://doi.org/10.1063/1.4802405

Mochizuki, H., 2022. Validation of neutronics and thermal-hydraulics coupling model of the RELAP5-3D code using the MSRE reactivity insertion tests. Nuclear Engineering and Design 389. https://doi.org/10.1016/j.nucengdes.2022.111669

Riley, B.J., McFarlane, J., DelCul, G.D., Vienna, J.D., Contescu, C.I., Forsberg, C.W., 2019. Molten salt reactor waste and effluent management strategies: A review. Nuclear Engineering and Design. https://doi.org/10.1016/j.nucengdes.2019.02.002

Robertson, R.C., 1965. MSRE Design and Operations Report Part I Description of Reactor Design. Oak Ridge National Laboratory, ORNL-TM-728. https://doi.org/10.2172/4654707

Serp, J., Allibert, M., Beneš, O., Delpech, S., Feynberg, O., Ghetta, V., Heuer, D., Holcomb, D., Ignatiev, V., Kloosterman, J.L., Luzzi, L., Merle-Lucotte, E., Uhlíř, J., Yoshioka, R., Zhimin,

768 D., 2014. The molten salt reactor (MSR) in generation IV: Overview and perspectives.
769 Progress in Nuclear Energy 77, 308–319. https://doi.org/10.1016/j.pnucene.2014.02.014
770 Spriggs, G.D., Campbell, J.M., Piksaikin, V.M., 2002. An 8-group Delayed Neutron Model Based
771 on a Consistent Set of Half-Lives. Progress in Nuclear Energy 41, 223–251.
772 https://doi.org/10.1016/S0149-1970(02)00013-6
773 Steffy R. C., Wood P. J., 1969. Theoretical Dynamic Analysis of the MSRE with 233U Fuel. Oak
774 Ridge National Laboratory, ORNL-TM-2571. https://doi.org/10.2172/4771215
775 Tuttle, R.J., 1975. Delayed-Neutron Data for Reactor-Physics Analysis. Nuclear Science and
776 Engineering 56, 37–71. https://doi.org/10.13182/nse75-a26620
777 Wooten, D., Powers, J.J., 2018. A Review of Molten Salt Reactor Kinetics Models. Nuclear
778 Science and Engineering 191, 203–230. https://doi.org/10.1080/00295639.2018.1480182
779 Wu, J., Chen, J., Cai, X., Zou, C., Yu, C., Cui, Y., Zhang, A., Zhao, H., 2022. A Review of Molten
780 Salt Reactor Multi-Physics Coupling Models and Development Prospects. Energies (Basel).
781 https://doi.org/10.3390/en15218296
782 Zanetti, M., Cammi, A., Fiorina, C., Luzzi, L., 2015. A Geometric Multiscale modelling approach
783 to the analysis of MSR plant dynamics. Progress in Nuclear Energy 83, 82–98.
784 https://doi.org/10.1016/j.pnucene.2015.02.014
785 Zanetti, M., Luzzi, L., Cammi, A., Fiorina, C., 2014. An Innovative Approach to Dynamics
786 Modeling and Simulation of the Molten Salt Rector Experiment, in: PHYSOR 2014 - The
787 Role of Reactor Physics Toward a Sustainable Future. Kyoto, Japan.
788 Zuo, X. Di, Cheng, M.S., Dai, Y.Q., Yu, K.C., Dai, Z.M., 2022. Flow field effect of delayed neutron
789 precursors in liquid-fueled molten salt reactors. Nuclear Science and Techniques 33.
790 https://doi.org/10.1007/s41365-022-01084-0

Appendices

The DNPs group parameters used in the simulations were based on published data for the MSRE and thermal neutron fission of ^{233}U. Table A.1 presents the six-group delayed neutron parameters for the MSRE used in the reduced DNPs models. Table A.2 provides the eight-group delayed neutron parameters derived from the thermal neutron fission of ^{233}U used in the expanded DNPs models.

Table A.1. Six-group delayed neutron group parameters for the MSRE used in the reduced DNPs models (Steffy R. C. and Wood P. J., 1969).

Group, i	Half-life, $T_{1/2,\,i}$ (s)	Effective delayed neutron fraction, $\beta_{eff,\,i}$
1	55.01	0.000228
2	20.57	0.000788
3	4.987	0.000664
4	2.132	0.000736
5	0.613	0.000136
6	0.277	0.000088

807 Table A.2. Eight-group delayed neutron group parameters in thermal neutron Fissioning of ^{233}U

808 used in the expanded DNPs models (Spriggs et al., 2002).

Group	Half-life (s)	Relative abundance
1	55.6	7.97E-02
2	24.5	1.67E-01
3	16.3	1.50E-01
4	5.21	2.00E-01
5	2.37	2.98E-01
6	1.04	3.88E-02
7	0.424	5.60E-02
8	0.195	1.05E-02

809

810

811

812